SUPPLEMENTARY APPENDIX

HIF1A is a critical downstream mediator for hemophagocytic lymphohistiocytosis

Rui Huang,[1,2] Yoshihiro Hayashi,[1,3] Xiaomei Yan,[1] Jiachen Bu,[1,4] Jieyu Wang,[1] Yue Zhang,[1,5] Yile Zhou,[1] Yuting Tang,[1,6] Lingyun Wu,[1] Zefeng Xu,[5] Xin Liu,[4,7] Qianfei Wang,[4,7] Jianfeng Zhou,[6] Zhijian Xiao,[5] James P. Bridges,[8] Rebecca A. Marsh,[9] Kejian Zhang,[10] Michael B. Jordan,[9] Yuhua Li[2] and Gang Huang[1]

RH and YH contributed equally to this work and GH and YHL contributed equally to this study as joint senior authors

[1]Division of Experimental Hematology and Cancer Biology, Cincinnati Children's Hospital Medical Center, OH, USA; [2]Department of Hematology, Zhujiang Hospital, Southern Medical University, Guangzhou, China; [3]Laboratory of Oncology, School of Life Sciences, Tokyo University of Pharmacy and Life Sciences, Japan; [4]Key Laboratory of Genomic and Precision Medicine, Beijing Institute of Genomics, Chinese Academy of Sciences, China; [5]State Key Laboratory of Experimental Hematology, Institute of Hematology and Blood Diseases Hospital, Chinese Academy of Medical Sciences & Peking Union Medical College, Tianjin, China; [6]Department of Hematology, Tongji Hospital, Tongji Medical College, Huazhong University of Science and Technology, Wuhan, Hubei, China; [7]University of Chinese Academy of Sciences, Beijing, China; [8]Perinatal Institute, Division of Pulmonary Biology, Cincinnati Children's Hospital Medical Center, OH, USA; [9]Division of Bone Marrow Transplantation and Immune Deficiency, Cincinnati Children's Hospital, OH, USA and [10]Division of Human Genetics, Cincinnati Children's Hospital Medical Center, OH, USA

 doi:10.3324/haematol.2017.174979

Received: June 20, 2017.

Accepted: August 24, 2017.

Pre-published: August 31, 2017.

Correspondence: gang.huang@cchmc.org

Supplementary Methods

Antibodies and reagents

Fluorochrome-conjugated anti-mouse antibodies were purchased from the indicated resource: APC-Cy7 conjugated anti-Gr1(Biolegend, Catalog No. 108424), PE conjugated anti- CD115 (Biolegend, Catalog No. 135505), APC conjugated anti-F4/80 (Biolegend, Catalog No. 123115), Pacific blue conjugated anti-CD80 (Biolegend, Catalog No. 104723), PE-Cy7 conjugated anti-CD206 (Biolegend, Catalog No.141719), APC conjugated anti-CD3 (eBioscience, Catalog No. 17-0032-82), PE conjugated anti-CD4 (eBioscience, Catalog No.12-0042-81), APC-Cy7 conjugated anti-CD8 (Biolegend, Catalog No. 100713), APC conjugated anti-NK1.1(eBioscience, Catalog No.17-5941-81), eFluor450 conjugated anti-DX5 (eBioscience, Catalog No.48-5971-80), Dylight 405 conjugated anti-HIF1A (Novus, Catalog No. NB100-479V), PE-Cy7 conjugated anti-CD107a (Biolegend, Catalog No. 121619), PE-Cy7 conjugated anti-NKp46 (eBioscience, Catalog No. 25-3351-80), Pacific Blue conjugated anti-IFN-γ (Biolegend, Catalog No. 505817), Pacific Blue Rat IgG1κ isotype (Biolegend, Catalog No. 400419). Anti-HIF1A (Novus, Catalog No. NB100-449) antibody was used for Western blot at a dilution of 1:1000. CpG1826 oligonucleotide with phosphorothioate modification was synthesized by IDT. Fixation/Permeabilization buffer for intracellular IFN-γ staining and transcription factor buffer for intracellular HIF1A staining were purchased from BD Bioscience. LCMV-infected *Prf1*$^{-/-}$ mouse model was generated as described[1]. Briefly, *Prf1*$^{-/-}$ mice were infected with LCMV-WE of 200 plaque-forming units (PFU) via intraperitoneal injection. Mice were sacrificed for analysis at 14 days after inoculation. Repeated CpG-treated mouse model was generated as described[2, 3]. Briefly, 75 μg of CpG DNA was injected intraperitoneally to wild type mice on day 0, 2, 4, 6, 8. On day 9, peripheral blood was sampled from retro-orbit after anesthesia. A complete blood count was performed on a Hemavet analyzer. Then mice were euthanized and organs were taken for analysis.

Bioinformatic analysis

Two published microarray data from PBMCs of FHL patients and healthy donors (GSE26050) and sJIA patients and healthy donors (GSE7753) were analyzed[4, 5]. Transcription factor-target enrichment analysis was performed by the software of AltAnalyze (version 2.1.0)[6]. Differentially expressed genes between patients and healthy donors were selected based on a fold change > 1.5 and $p < 0.05$ in AltAnalyze. GSEA was performed to analyze enrichment of HIF1A signature in FHL and SJIA dataset. Upregulated genes with fold change more than 2.0 in HIF1A transduced $CD34^+$ human cord blood compared to empty vector transduced cells from a published microarray data (GSE54663) were used as the HIF1A induced gene set. The overlapped leading edge genes from GSEA analysis to FHL and sJIA datasets were analyzed online (http://bioinfogp.cnb.csic.es/tools/venny/index.html). Gene ontology analysis to the overlapped leading edge genes was performed online (https://david.ncifcrf.gov).

Flow cytometry

Single cells were separated and suspended from peripheral blood, bone marrow, spleen, and liver. Cell surface markers were stained with standard protocols. For intracellular IFN-γ staining, splenocytes were separated from mice and incubated with 10 ng/ml PMA, 750 ng/ml ionomycin, and GolgiStop (Monensin) at 37 °C for 4-5 h. After wash, cell surface markers were stained followed by fixation and permeabilization. Then intracellular IFN-γ was stained using anti- IFN-γ monoclonal antibody and isotype antibody. For cell surface CD107a staining, splenocytes were separated and were restimulated with PMA, ionomycin, and GolgiStop at the same concentration as mentioned above along with anti-CD107a monoclonal antibody for 5 h. Then, cells were

washed and stained with other cell surface markers. Intracellular HIF1A staining was performed with Dylight 405 conjugated anti-HIF1A antibody (Novus, Catalog No. NB100-479V) following cell surface staining and subsequent fixation and permeabilization by transcription factor buffer (BD Biosciences). Flow cytometric analysis was performed using FACS Canto II (BD Biosciences). Data were analyzed by FlowJo version 10.1.1 (Tree Star, Ashland, OR).

ELISA

Multi-Analyte Elisa Array kit was purchased from Qiagen (Catalog No. 336161), mouse ferritin ELISA kit was purchase from Abcam (Catalog No. ab157713), and used according to the manufacturer's instructions.

Western Blot

Whole cell extract was prepared by lysing cells in a 2×sodium dodecyl sulfate (SDS) sample buffer containing 0.2 mM Na_3VO4, 10 mM NaF, 1mM phenylmethylsulfonyl fluoride (Sigma-Aldrich), 10 mM β-Glycerophosphate, 2.5 mM dithiothreitol, 5% 2-mercaptoethanol, 1 mM 4-Amidinophenylmethanesulfonyl Fluoride Hydrochloride (Sigma-Aldrich), and proteinase inhibitors (Sigma-Aldrich, Roche Diagnosis) followed sonication. Samples were boiled at 95 °C for 10 minutes and loaded to SDS-polyacrylamide gel electrophoresis (PAGE) and electrotransferred to polyvinylidene fluoride (PVDF) membranes (Millipore). The following primary antibodies were used: anti-HIF1A (NB100-449, Novus), anti-β-Actin (sc-1616R, Santa Cruz). Horseradish peroxidase-conjugated antibody to rabbit (NA934V, GE Healthcare) was used as the secondary antibody. Super Signal West Dura Chemiluminescent Substrate (Pierce) was used for ECL detection. ImageJ software was used for quantification.

Histology

Liver, spleen, and femur or sternum were fixed in formalin and embedded in paraffin. Organs were sectioned and stained with hematoxylin and eosin (H&E). Images were captured using Motic BA310 biological lab microscope with Motic Image Plus 2.0 software at an original magnification of ×400.

Generation of bone marrow derived macrophages

Cells were harvested from bone marrow and cultured at a concentration of 1×10^6/ml in DMEM F12 complete medium containing 20 ng/ml M-CSF in 37 °C, 5% CO_2 incubator. Change medium every 3 days. IFN-γ (final concentration as 20 ng/ml) or IL-4 (final concentration as 20 ng/ml) were added to culture medium for 24 h to generate type 1 or type 2 polarized macrophages.

Assay to determine the capacity of macrophages to engulf erythroblasts

Preparation of erythroblasts was previously described[7]. Briefly, 0.5 ml blood was withdrawn from mice. Four days later, cells were harvested from the mice's spleen and passed through a mesh, erythroblasts were collected by density gradient centrifugation on 70% Percoll and added to incubate with macrophages for 12 h. Cytospin was prepared followed by Giemsa staining. Engulfment of erythroblasts by macrophages was observed under microscope. Three random fields were captured at ×100 magnification, the percentage of macrophages engulfing erythroblasts in total macrophages was determine.

1. Jordan MB, Hildeman D, Kappler J, Marrack P. An animal model of hemophagocytic lymphohistiocytosis (HLH): CD8+ T cells and interferon gamma are essential for the disorder. Blood. 2004;104(3):735-743.

2. Behrens EM, Canna SW, Slade K, et al. Repeated TLR9 stimulation results in macrophage activation syndrome-like disease in mice. J Clin Invest. 2011;121(6):2264-2277.

3. Das R, Guan P, Sprague L, et al. Janus kinase inhibition lessens inflammation and ameliorates disease in

murine models of hemophagocytic lymphohistiocytosis. Blood. 2016;127(13):1666-1675.
4. Sumegi J, Barnes MG, Nestheide SV, et al. Gene expression profiling of peripheral blood mononuclear cells from children with active hemophagocytic lymphohistiocytosis. Blood. 2011;117(15):e151-160.
5. Fall N, Barnes M, Thornton S, et al. Gene expression profiling of peripheral blood from patients with untreated new-onset systemic juvenile idiopathic arthritis reveals molecular heterogeneity that may predict macrophage activation syndrome. Arthritis Rheum. 2007;56(11):3793-3804.
6. Emig D, Salomonis N, Baumbach J, Lengauer T, Conklin BR, Albrecht M. AltAnalyze and DomainGraph: analyzing and visualizing exon expression data. Nucleic Acids Res. 2010;38(Web Server issue):W755-762.
7. Yoshida H, Kawane K, Koike M, Mori Y, Uchiyama Y, Nagata S. Phosphatidylserine-dependent engulfment by macrophages of nuclei from erythroid precursor cells. Nature. 2005;437(7059):754-758.

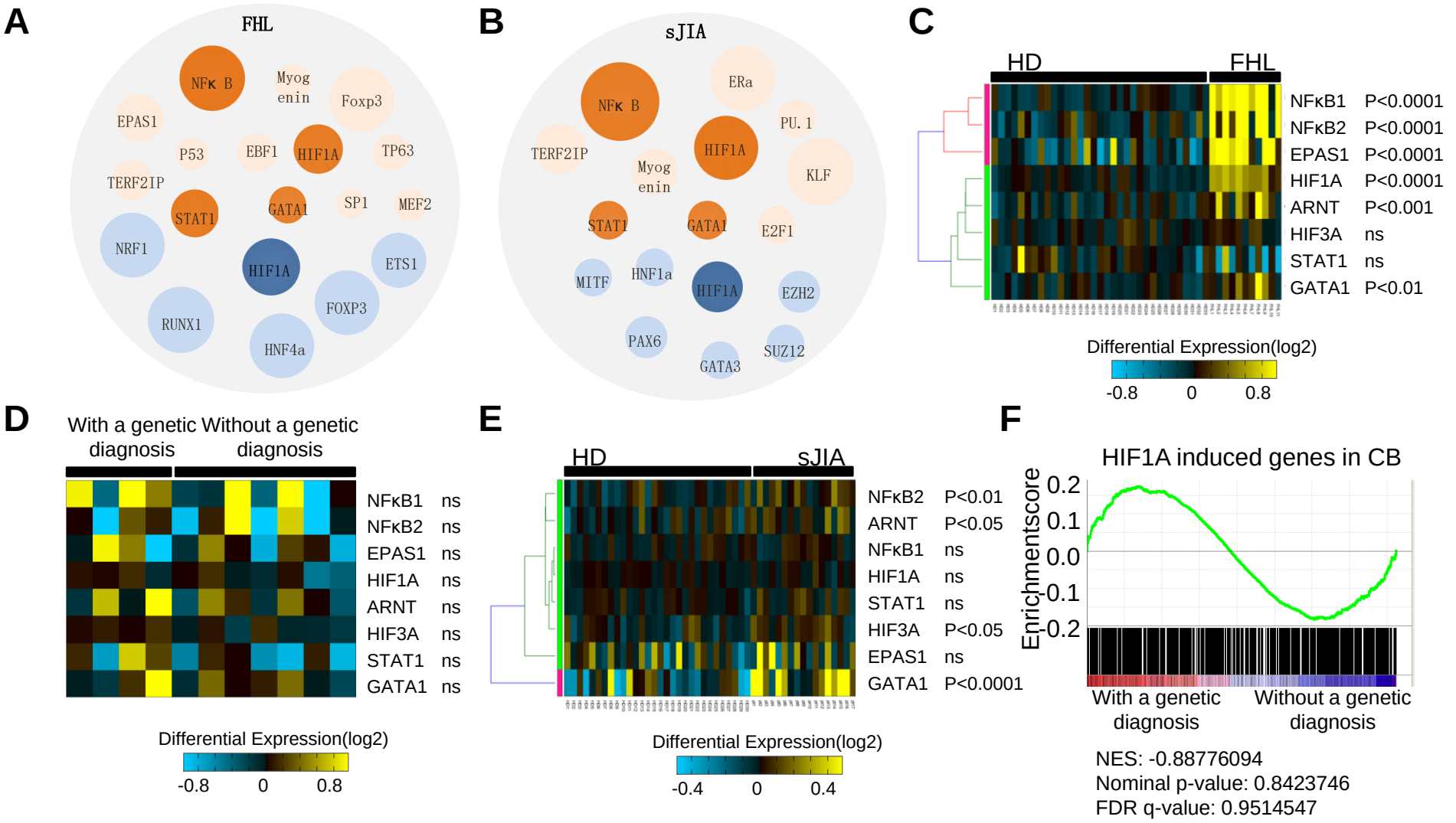

Supplementary Figure S1. HIF1A cooperates with multiple transcription factors to play a role in HLH. (A-B) FHL and sJIA datasets were analyzed by AltAnalyze software. Schematic diagrams of predicted top transcription factors involved in FHL (A) and sJIA (B) were shown. The size of the indicated transcription factor is related to the number of its target genes in HLH. (C-E) Heatmaps of indicated transcription factors in FHL patients versus healthy donors (C), FHL patients with versus without a genetic diagnosis (D), sJIA patients versus healthy donors (E) were shown. (F) GSEA plot showing no significant difference of HIF1A signature enrichment between FHL patients with and without a genetic mutation. ns: non-significant.

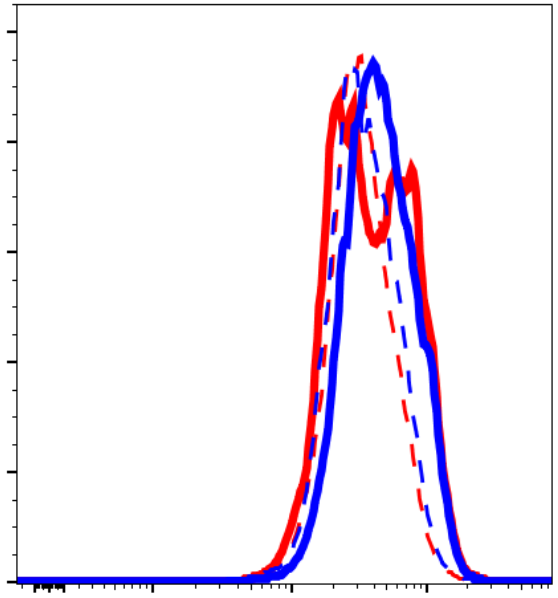

Supplementary Figure S2. *Vav1*-Cre/LSL/TPM mice have comparable level of HIF1A with CpG injected C57/B6 mice. Doxycycline was administrated to *Vav1*-Cre/LSL/TPM and *Vav1*-Cre/LSL/WT, CpG or PBS was injected i.p. to wild-type mice. On day 5 after doxycycline and day 9 after CpG initiation, mice were sacrificed and analyzed. Representative cytometry flow plot showing HIF1A level in splenic macrophages in indicated mice (Gated on $Gr1^{-}CD115^{-}F4/80^{+}SSC^{low}$).

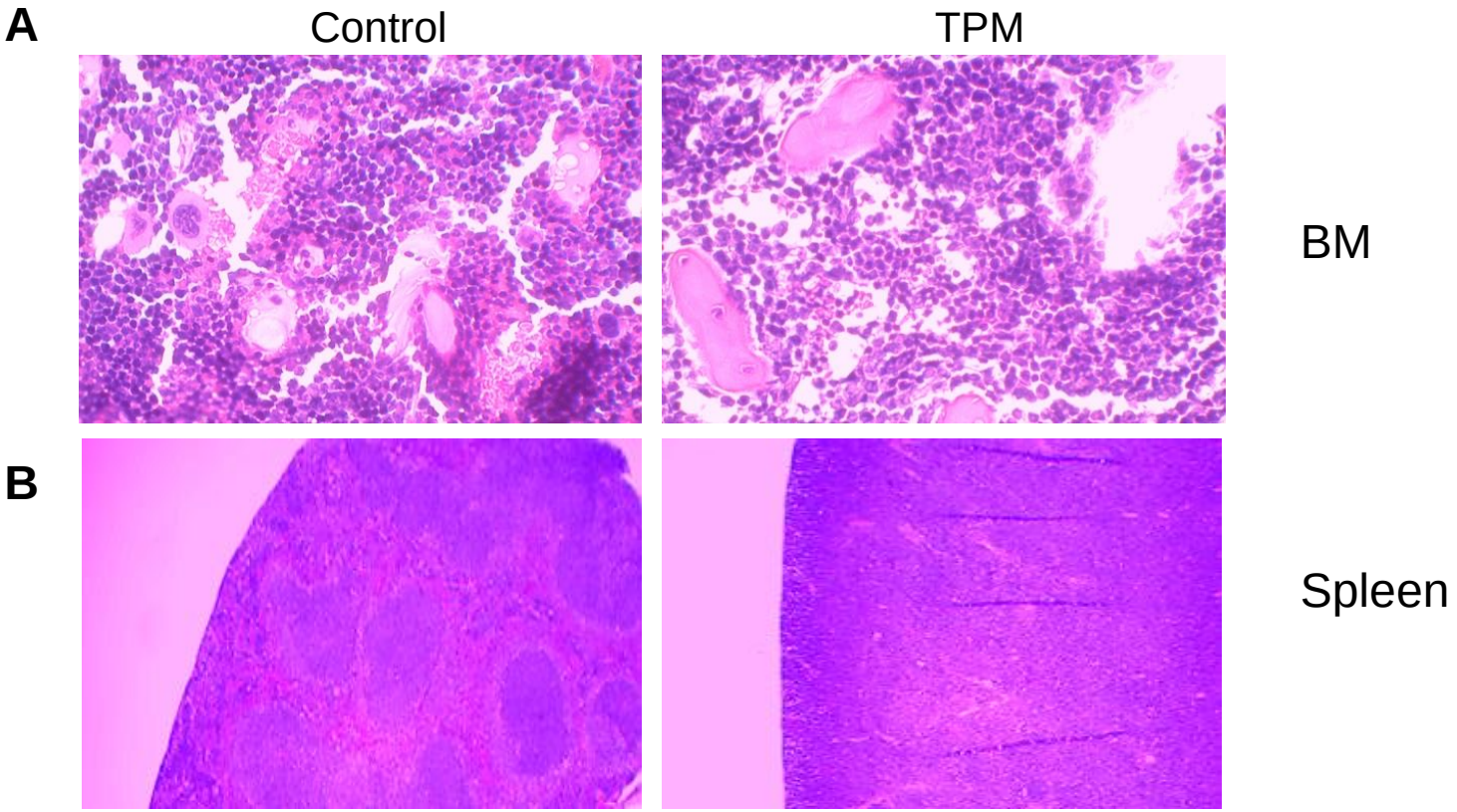

Supplementary Figure S3. Induction of HIF1A/ARNT allele in hematopoietic cells reduces bone marrow cellularity, and disrupts normal splenic structure in C57/B6 mice. (A) Representative sections of bone marrow from *Vav1*-Cre/TPM mouse, and control mouse at an original magnification of × 400. (B) Representative sections of spleen from *Vav1*-Cre/TPM mouse, and control mouse at an original magnification of × 400.

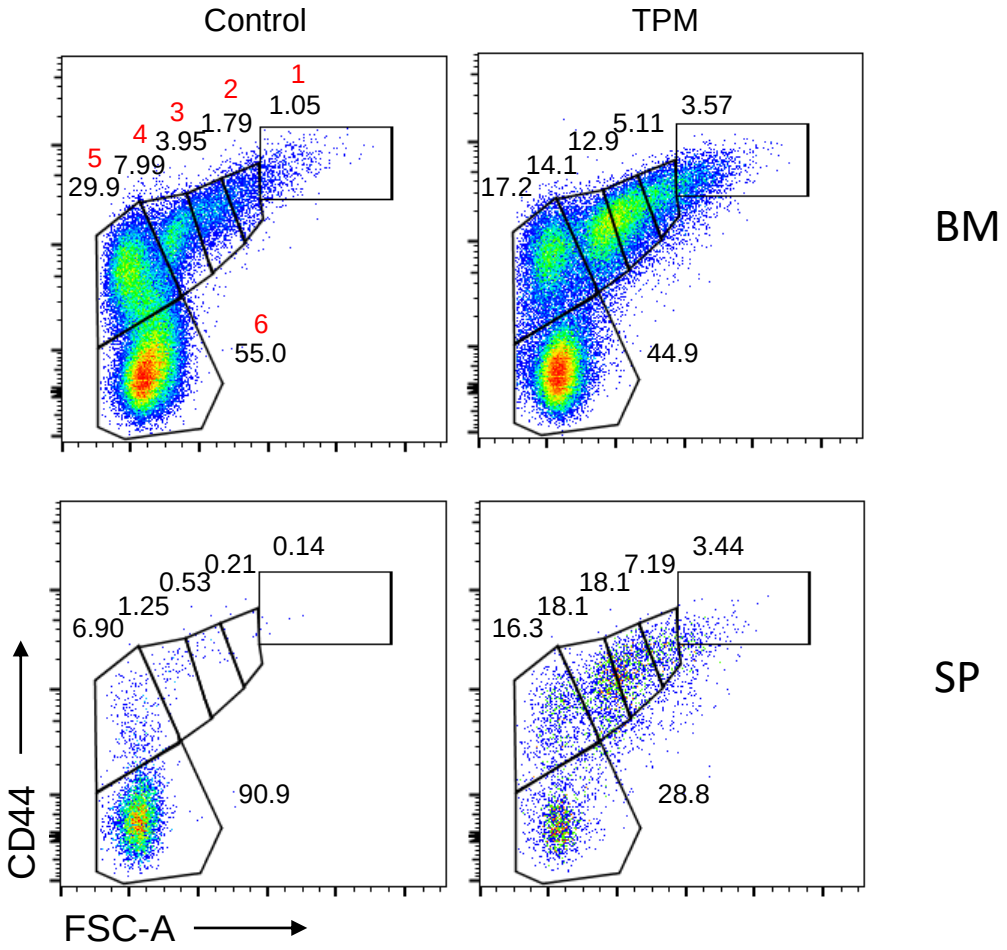

Supplementary Figure S4. Vav1-Cre/TPM mice have robust erythropoiesis in bone marrow and spleen. Representative of flow cytometry dot plots showing differentiation of erythrocytes in bone marrow and spleen after doxycycline induction in *Vav1*-Cre/TPM mice and control mice. 1-6 in dot plot of CD44 versus FSC indicates proerythroblasts, basophilic erythroblasts, polychromatic erythroblasts, orthochromatic erythroblasts, reticulocytes, and mature red cells, respectively.

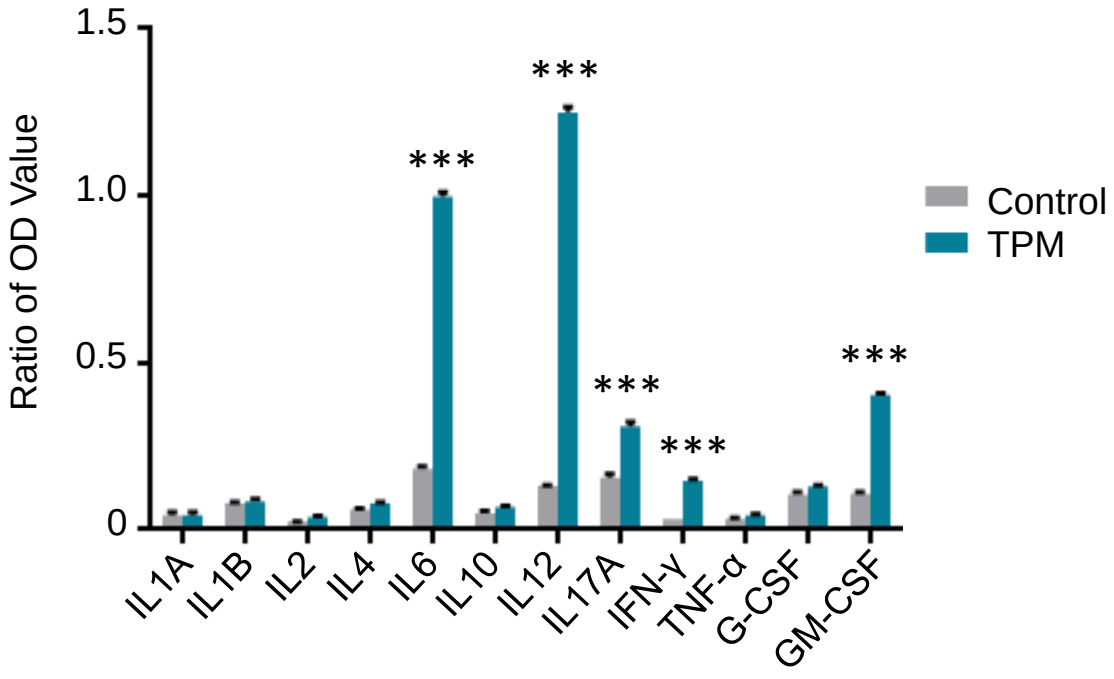

Supplementary Figure S5. Serum cytokines and chemokines are elevated in TPM induced mice. Serum of 6 *Vav1*-Cre/TPM and control mice was pooled, respectively. Indicated cytokines and chemokines were measured by ELISA. The ratio of OD value of *Vav1*-Cre/TPM mice over control mice was shown.

A

Chemokines	Inhibit HIF1A
CXCL2 CXCL16 CCL23	CITED2
Nucleoporin	**Apoptosis**
NUP98	BCL2L1
Macrophage activation	**Others**
THBS1	PPP1R15A GADD45A STAT3 BNIP3L CD82 PICALM ADM
Glycolysis	
PGK1 HK2 SLC2A3 PFKFB3 PKM2	

(HIF1A direct targets in blue)

B

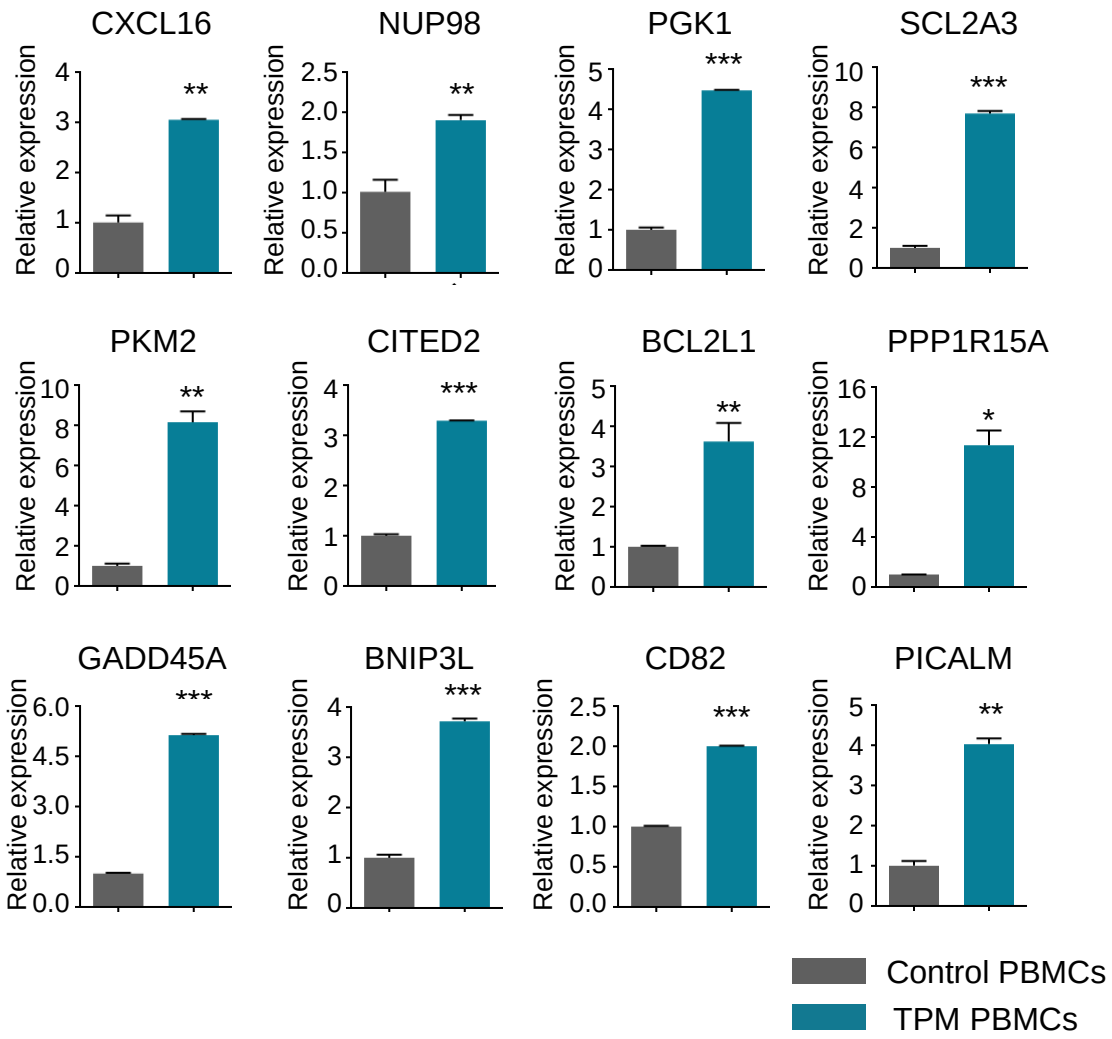

Supplementary Figure S6. Expression of genes in overlapped leading edge genes of GSEA from FHL and sJIA datasets are increased in peripheral blood of TPM induced mice. (**A**) Table showing 19 validated genes from overlapped leading edge genes of GSEA from FHL and sJIA datasets. The known HIF1A direct target genes are marked blue. (**B**) Relative mRNA expression of indicated genes was measured by qRT-PCR in PBMCs of *Vav1*-Cre/TPM mice and control mice.

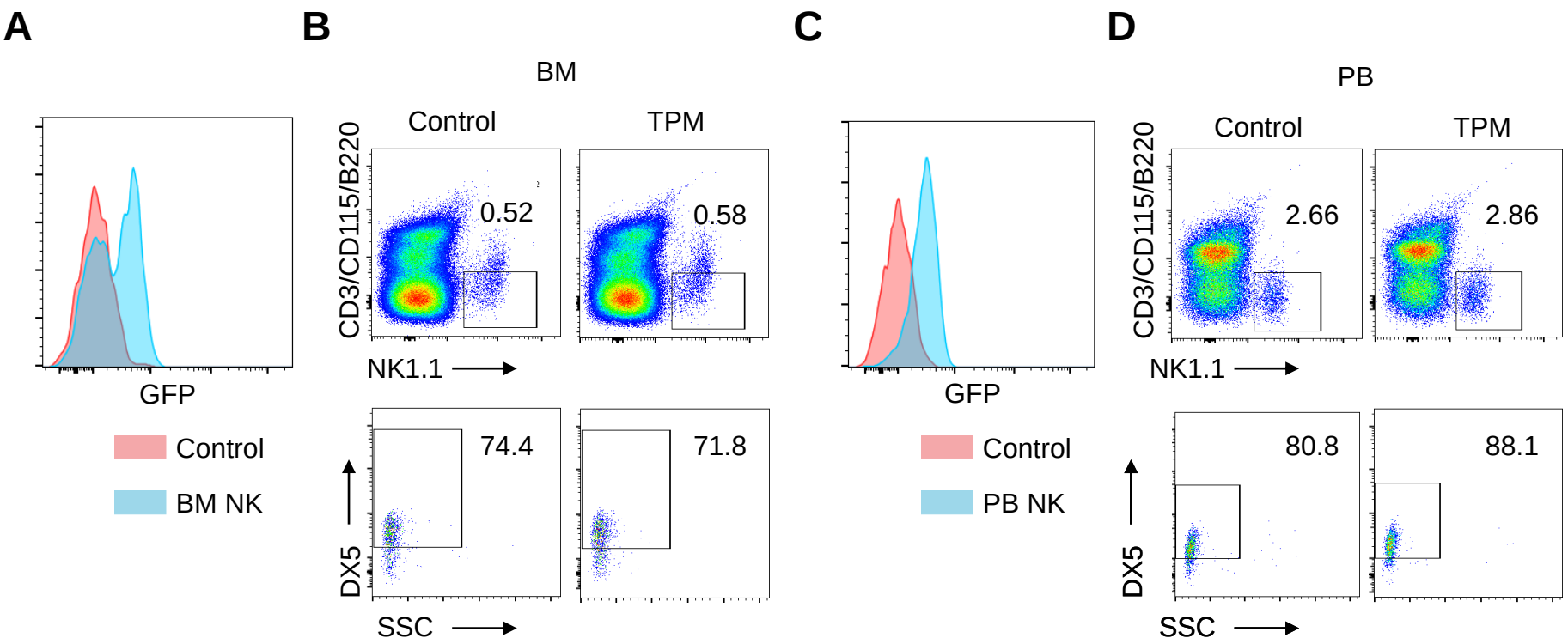

Supplementary Figure S7. Intrinsic induction of TPM/ARNT in NK cells does not change the percentage of total NK cells and mature NK cells in bone marrow and peripheral blood. *Ncr1*-iCre/LSL/TPM mice were generated, LSL/TPM mice were served as control. *Ncr1*-iCre /LSL/TPM mice and LSL/TPM mice were administrated with doxycycline. (A, C) GFP in NK cells was shown in bone marrow (A) and peripheral blood (C). (B, D) Representative flow cytometry dot plots show total NK cells and mature NK cells in bone marrow (B) and peripheral blood (D).

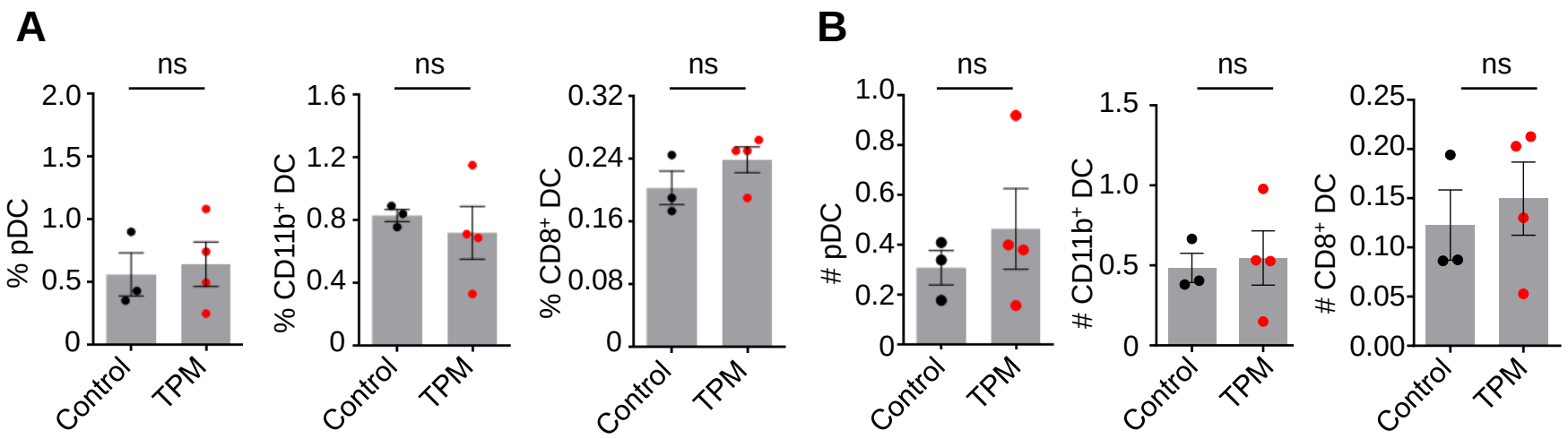

Supplementary Figure S8. The number of dendritic cells does not change at a late stage in TPM induced mice. *Vav1*-Cre/TPM and control mice were administrated with doxycycline. The percentage (A) and absolute number (B) of pDC, CD11b$^+$cDC, and CD8$^+$cDC in spleen on day 6 after doxycycline induction were shown. #: absolute number. ns: non-significant.

A

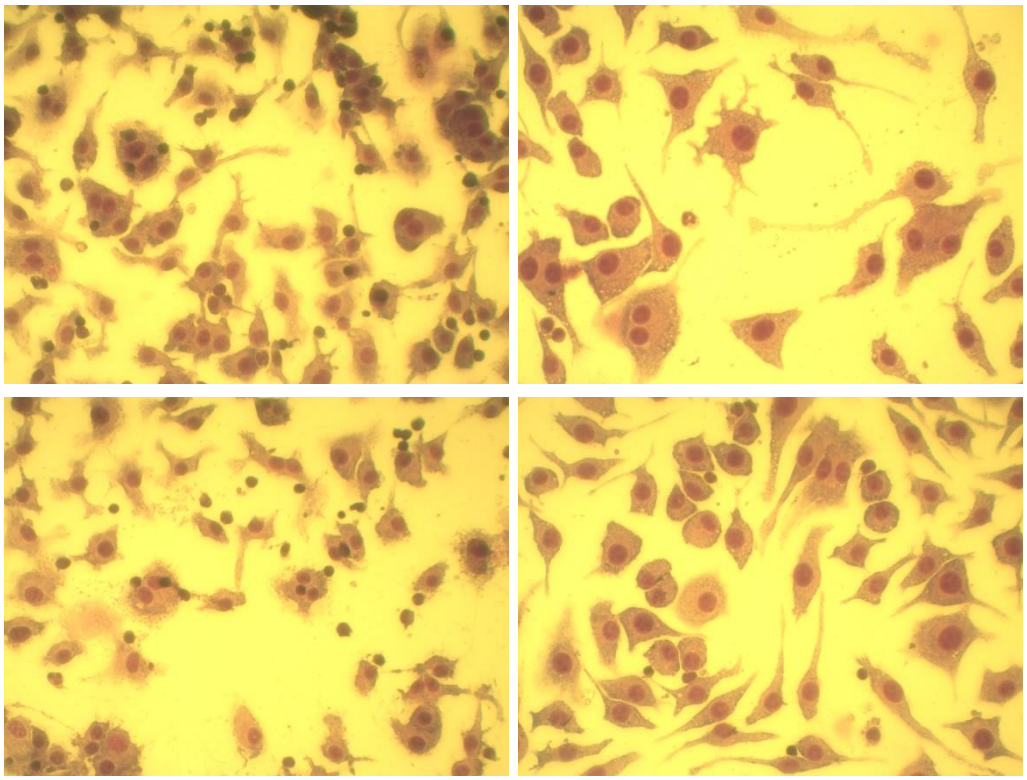

B

	without erythro (%)	with 1 erythro (%)	with 2 erythro (%)	with 3 erythro (%)	with 4 erythro (%)	with erythro (%)	P value*
type1Φ	84.44±0.59	11.99±2.17	2.56±2.56	0.51±0.51	0.51±0.51	15.56±0.59	
type2Φ	100.0±0.0	0.0±0.0	0.0±0.0	0.0±0.0	0.0±0.0	0.0±0.0	<0.0001

Supplementary Figure S9. IFN-γ polarized type 1 macrophages engulf erythroblasts in vitro. (A) Representative plots showing IFN-γ polarized type 1 macrophages (left) rather than IL-4 polarized type2 macrophages (right) engulfing erythroblasts. (B) Table showing quantitation of polarized macrophages engulfing erythroblasts. * indicates P value between percentage of type 1 polarized macrophages with erythroblasts and that of type 2 polarized macrophages with erythroblasts.

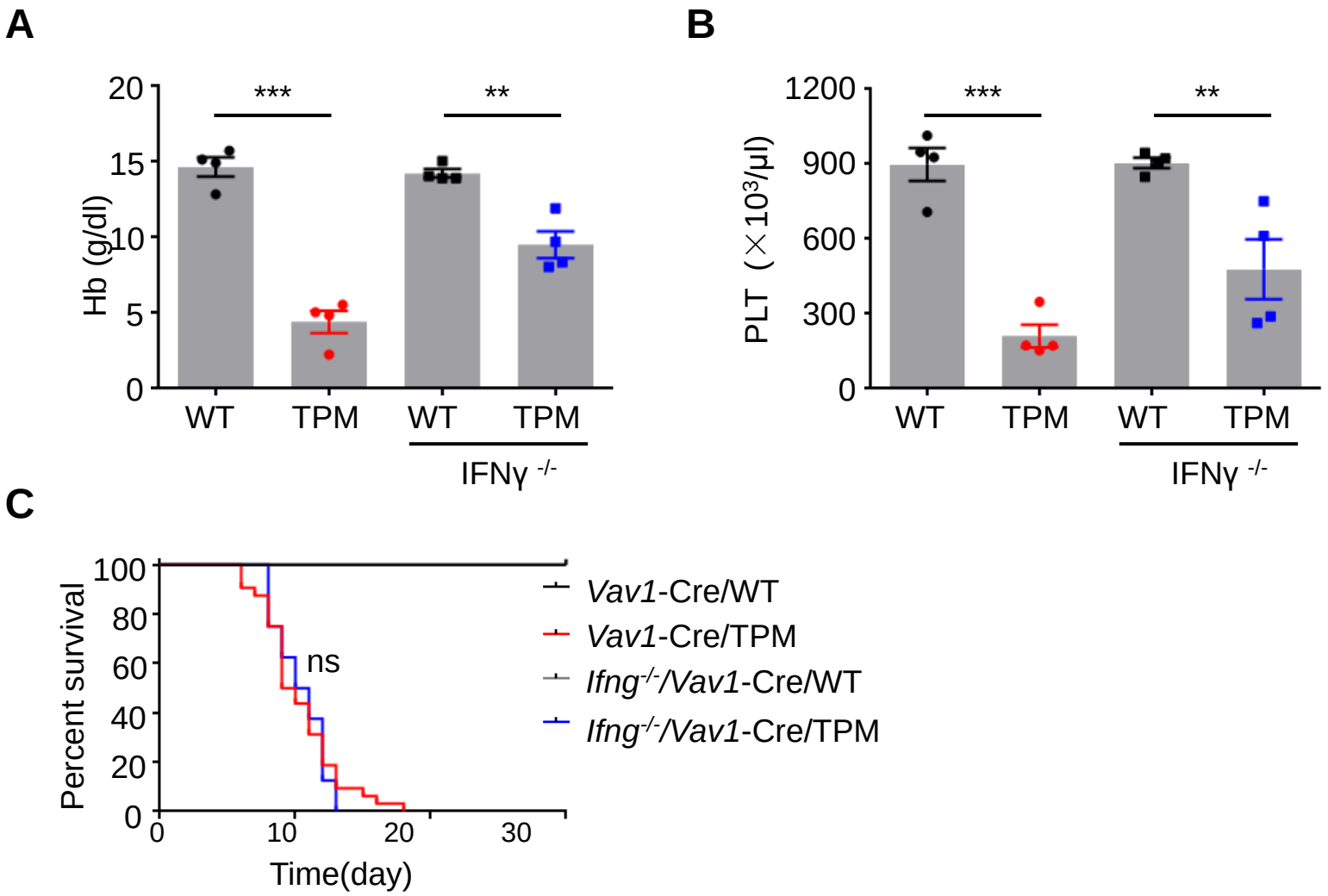

Supplementary Figure S10. Most of the TPM/ARNT induced HLH like phenotypes cannot be rescued in IFN-γ deficient mice. *Ifng*$^{-/-}$/*Vav1*-Cre/LSL/TPM (*Ifng* $^{-/-}$/TPM) mice were generated. *Ifng*$^{-/-}$/*Vav1*-Cre/LSL/WT (*Ifng* $^{-/-}$/WT) mice served as their control. *Ifng*$^{-/-}$/TPM, *Ifng*$^{-/-}$/WT, *Vav1-Cre*/TPM, *Vav1*-Cre/WT mice were administrated with doxycycline. (A-B) Hemoglobin (A) and platelets (B) on day 8 after doxycycline induction were shown. (C**)** Kaplan-Meier analysis of survival of *Ifng*$^{-/-}$/TPM (n=8), *Ifng*$^{-/-}$/WT (n=8), *Vav1-Cre*/TPM (n=32), *Vav1*-Cre/WT (n=26) mice was shown. Statistics analysis showed that there was a significant difference between *Ifng*$^{-/-}$/TPM and *Ifng*$^{-/-}$/WT mice (P<0.0001), but no significant difference between *Ifng*$^{-/-}$/TPM and *Vav1-Cre*/TPM mice (P>0.05).